

## BRACKETT-ALPHA LINE PROFILES OF YOUNG STELLAR OBJECTS

S. E. PERSSON,<sup>1, 2, 3</sup> T. R. GEBALLE,<sup>1, 2, 3, 4</sup> PETER J. MCGREGOR,<sup>1</sup> SUZAN EDWARDS,<sup>3, 5</sup>  
AND CAROL J. LONSDALE<sup>2, 3, 6</sup>*Received 1984 March 5; accepted 1984 May 4*

## ABSTRACT

Profiles of the Br $\alpha$  line of H I at a velocity resolution of 45 km s<sup>-1</sup> are presented for the compact embedded infrared objects BN, S106/IRS 3, GL 490, GL 961, GL 989, Mon R2/IRS 2, and for the visible objects LkH $\alpha$  101, T Tau, and R Mon. All the objects have wide lines, with full widths at half-maximum ranging from 60 to 235 km s<sup>-1</sup>. There is some variation in the characteristic shapes of the line profiles, but only BN and S106/IRS 3 show evidence for asymmetry; both objects display a weak enhancement of the blue side of the line with respect to the red.

A proportionality between Br $\alpha$  luminosity and bolometric luminosity, analogous to that found by Thompson for Br $\gamma$  luminosities, is shown to extend over three orders of magnitude for these young stellar objects. This finding supports the idea that the physical conditions and gas motions in the circumstellar envelopes of young stellar objects are closely related over a large range in luminosity. The Br $\alpha$  line strengths are compared to radio continuum flux densities in the context of stellar wind models. Fair agreement is found for the Simon *et al.* formulation, in nearly all cases. Momentum deposition rates deduced from Br $\alpha$  or radio continuum fluxes are consistent with those available in the radiation fields, which therefore appear capable of driving the ionized gas outflows in the immediate vicinities of the core sources.

A comparison is made between the H $\alpha$  and Br $\alpha$  profiles for T Tau. The Br $\alpha$  line probably arises in the envelope of T Tau itself and not the binary companion T Tau(S) recently discovered by Dyck *et al.* Predictions of stellar wind models are consistent with the Br $\alpha$  and radio fluxes for T Tau(N) but not for T Tau(S), unless the Br $\alpha$  line for T Tau(S) is attenuated by an amount corresponding to  $A_V \sim 100$  mag.

*Subject headings:* infrared: spectra — stars: pre-main-sequence

## I. INTRODUCTION

The discovery of bright H I Br $\alpha$  line emission in the BN object by Grasdalen (1976) has led to intensive study of the phenomenon of hydrogen line emission from compact infrared objects in early evolutionary stages and embedded in molecular clouds. Searches in the 2  $\mu$ m region at intermediate spectral resolution ( $\lambda/\Delta\lambda \sim 2000$ ) by Thompson and collaborators (see Thompson 1981 for a review) and at Br $\alpha$  by Simon, Simon, and Joyce (1979), Joyce and Simon (1982), and Simon *et al.* (1983) have led to detections of H I line emission from a diverse collection of objects. Some of the more heavily obscured objects were thought at one time to be protostars, but the H I line detections led to the belief that the luminous infrared sources were ultracompact H II regions with exciting stars near the zero-age main sequence. However, a basic early result of these studies, and one emphasized by Thompson (1981, 1982), was that the Brackett line emission is often far stronger than expected for such an H II region, if Case B recombination

theory applies. Thus neither the protostar, compact H II region, nor ultracompact H II region designation seems appropriate for these objects. The term young stellar object (YSO), used for a wide variety of pre-main-sequence objects, is adopted here.

The H I lines in the few sources measured so far are substantially wider than those seen in compact H II regions. Velocity resolved spectroscopy of the Br $\gamma$  and Br $\alpha$  lines in BN (Scoville *et al.* 1983) and GL 490 and M17/IRS 1 (Simon *et al.* 1981) shows lines with full widths at half-maximum (FWHM) of  $\sim 150$  km s<sup>-1</sup>. These findings have led several authors to construct models for the H I emission that do not involve the Case B recombination assumption and that seek to explain the H I line widths and fluxes in terms of spherically symmetric outflowing winds (Krolik and Smith 1981; Simon *et al.* 1981, 1983, Scoville *et al.* 1983), in which the Brackett lines can attain substantial optical depth. These models are successful in reproducing the ratios of Brackett line to radio fluxes in a few sources (Bally and Predmore 1983). Recent observations in the 0.8–1.0  $\mu$ m region of many of the sources show that the Paschen lines are also optically thick (McGregor, Persson, and Cohen 1984). These data confirm that the H I line emission arises in a dense envelope that is in a state of highly supersonic motion and has a size scale of  $\sim 10^{13}$  cm. It is the nature of this envelope that is of interest—its density, state of ionization, degree of clumping, overall geometry, and velocity field are as yet poorly understood. The envelope physical conditions are also important to the problem of the origin of the extended cool molecular outflows observed from embedded infrared sources.

As only a few high-resolution profiles of infrared H I lines have appeared in the literature, we present here the initial

<sup>1</sup> Mount Wilson and Las Campanas Observatories of the Carnegie Institution of Washington.

<sup>2</sup> Observations were made at Palomar Observatory as part of a collaborative agreement between the Carnegie Institution of Washington and the California Institute of Technology.

<sup>3</sup> Visiting Astronomer at the Infrared Telescope Facility which is operated by the University of Hawaii under contract to the National Aeronautics and Space Administration.

<sup>4</sup> Kapteyn Astronomical Institutes, Rijksuniversiteit te Groningen, and United Kingdom Infrared Telescope.

<sup>5</sup> Five College Astronomy Department, Smith College.

<sup>6</sup> Department of Astronomy, University of California at Los Angeles, and Jet Propulsion Laboratory, California Institute of Technology.

results of a survey of the kinematics of the H I line-emitting gas in several other YSOs via high resolution spectroscopy of the Br $\alpha$  line. Our approach in this exploratory work has been to obtain kinematic information on sources in the compilation of Wynn-Williams (1982). Many of these sources are also known to be surrounded by high-velocity molecular outflows (Bally and Lada 1983; Edwards and Snell 1983).

## II. OBSERVATIONS

The spectra discussed in this paper were obtained with the Fabry-Perot/cold grating spectrometer described by Persson, Geballe, and Baas (1982) mounted on the Hale 5 m telescope on Palomar Mountain and on the IRTF at Mauna Kea Observatory. Spectra covering a velocity range greater than 1000 km s<sup>-1</sup> at the Br $\alpha$  line of H I at 4.05  $\mu$ m were obtained of the 11 sources listed in Table 1 plus the three radio continuum knots

associated with S106-S106A, B, and C (Israel and Felli 1976). A spectrum of the Br $\gamma$  line in S106/IRS 3<sup>7</sup> was also measured at a velocity resolution comparable to that of the Br $\alpha$  data.

### a) Palomar Observations

The Hale 5 m data were obtained in 1981 July. Conventional chopping and beam-switching techniques were used with an entrance aperture 4" in diameter, and a throw of 25" EW. The spectral resolution of the Fabry-Perot was set at 75 km s<sup>-1</sup> (FWHM Lorentzian) and the cold grating spectrometer band was 1500 km s<sup>-1</sup>. The rather low spectral resolving power of these early measurements was chosen to maximize the sensi-

<sup>7</sup> We shall henceforth refer to the bright near-infrared continuum source in S106 by the name originally given to it by Pipher *et al.* (1976), viz., S106/IRS 3, and not by the designation IRS 4 (Gehrz *et al.* 1982).

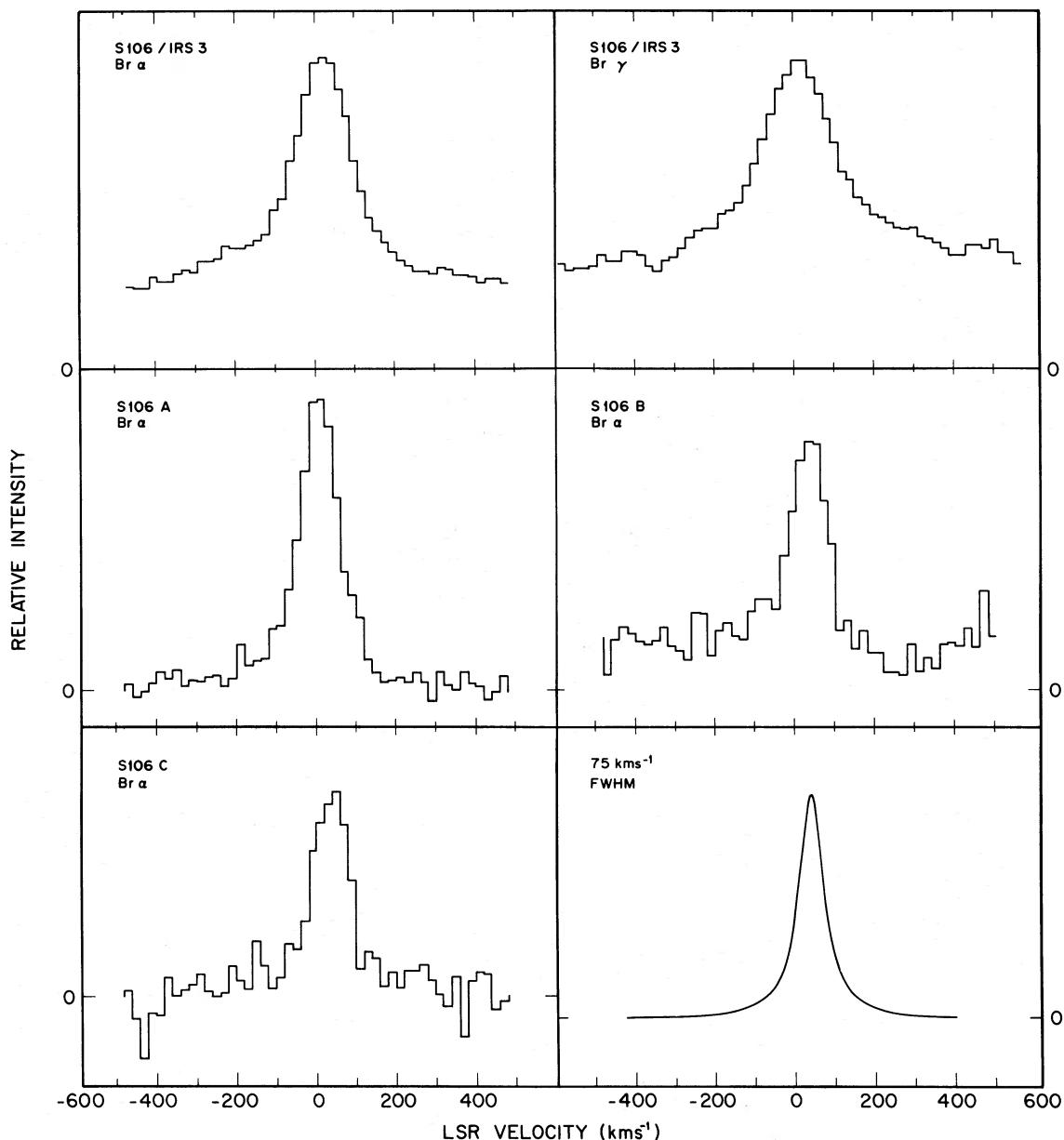


FIG. 1.—Fabry-Perot spectra of the Br $\alpha$  and Br $\gamma$  lines of H I in S106. The instrumental Lorentzian is shown in the lower right.

tivity to any broad and faint line wings that might be present. The velocity of peak transmission of the Fabry-Perot was monitored during each sweep by detecting and recording the reflected 6328 Å interference fringes from a He-Ne laser. Individual groups of four or eight scans were later reregistered in velocity to an accuracy better than  $5 \text{ km s}^{-1}$  and coadded. Figures 1 and 2 present the spectra of the four embedded sources and the three H II regions. Flux calibrations were not attempted because of the small projected beam size and the consequent sensitivity to seeing, guiding, and extinction variations. However, standard stars were measured to determine the spectral baseline shapes, the curvature of which arises from the convolution of the Fabry-Perot scan with the fixed spectral response profile of the grating spectrometer. The spectra in Figures 1 and 2 have been divided by these stellar spectra. For emission lines on strong continua, small changes in the starting point of the Fabry-Perot sweep with respect to the grating position between the object and standard star spectra, together with variations of the source location in the aperture, produce changes in the shape of the baseline, even after ratioing the object and standard spectra. These effects have caused sloping baselines in the ratioed spectra of M8E, GL 490, and M17/IRS 1 in Figure 2. Though annoying, this does not compromise the usefulness of the spectra for determining the characteristic shapes and centroids of the lines. Figure 1 also shows the instrumental resolution for the spectra in Figures 1 and 2. The noise level in each spectrum is best judged from the point-to-point variation in the baselines.

The measurements of S106B refer to a position that is a few arcsec N and E of the position given by Israel and Felli (1976). The VLA map of Bally, Snell, and Predmore (1983) indicates that our S106B position probably includes flux from gas to the north of the prominent dust lane.

#### b) IRTF Observations

The IRTF data were obtained in 1982 December. The entrance aperture was  $6''.5$  in diameter, and the chopper throw was  $20''$  except for S106/IRS 3 and Mon R2/IRS 2 where nearby sources could have confused the spectrum. A new technique was used in these measurements—the grating and Fabry-Perot were scanned together so that the peak of the Fabry-Perot transmission profile was always aligned with the peak of the grating profile over the total scan length of  $1000 \text{ km s}^{-1}$ . The spectral resolution of the Fabry-Perot was set to  $45 \text{ km s}^{-1}$ , and that of the grating spectrometer to  $450 \text{ km s}^{-1}$ . The simultaneous scanning and data recording functions were controlled by a microcomputer which also continuously monitored the alignment of the two passbands. Spectral baselines flat to better than  $\pm 5\%$  (peak to peak) resulted; the residual ripples due to variations in the response of the broad-band blocking filter were highly repeatable and were divided out of both the object and standard star spectra. Figure 3 displays the spectra (objects ratioed to standards) obtained in this manner. Velocity calibration was achieved by measuring IC 418 as a standard; its velocity with respect to the local standard of rest (LSR) was taken from Schneider *et al.* (1983). Again the noise can be judged from the dispersion in the baselines.

The total Br $\alpha$  flux of HL Tau was measured using the grating spectrometer at the IRTF; the result is  $7.6 \pm 1.0 \times 10^{-20} \text{ W cm}^{-2}$ . This value is used in comparison with other objects below.

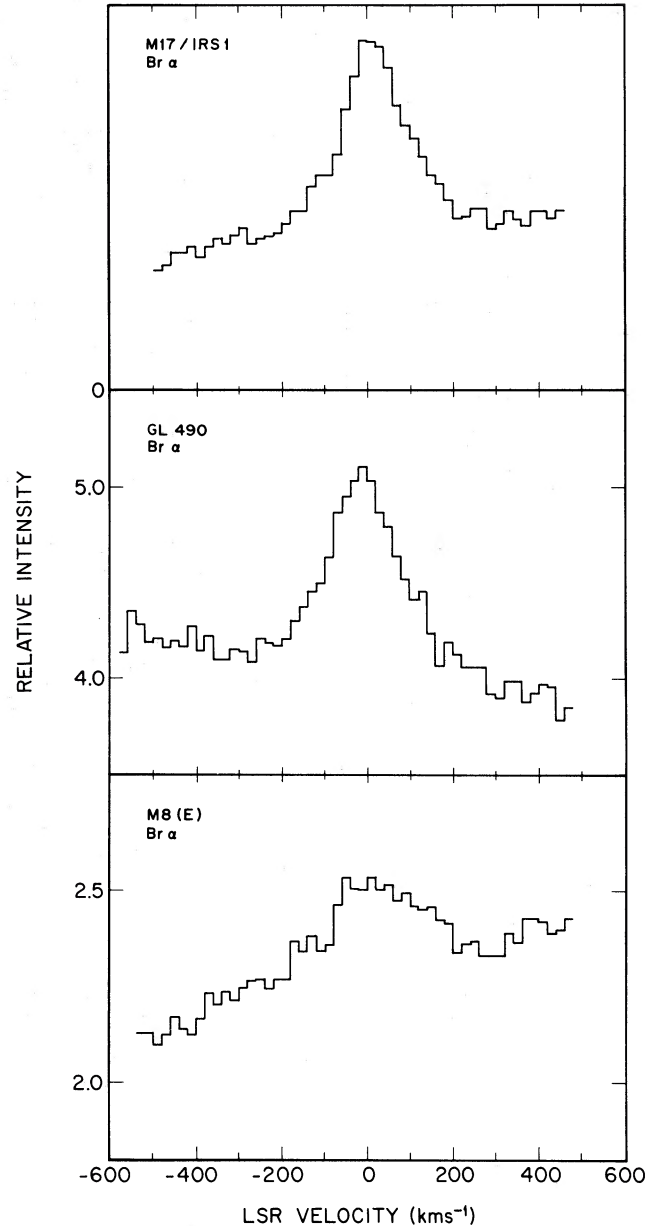


FIG. 2.—Fabry-Perot spectra of the Br $\alpha$  line of H I for three YSOs, obtained at  $75 \text{ km s}^{-1}$  resolution (same as Fig. 1). The sloping baselines are not real; see the text.

### III. RESULTS

#### a) Spectra

The results of the Fabry-Perot spectroscopy are displayed in Figures 1, 2, and 3, and Table 1 lists several observed and derived parameters of the sources. The equivalent widths ( $W_\lambda$ ) of the Br $\alpha$  lines are given in column (4). These values were obtained by integrating the flux density in the line out to a continuum level determined near the ends of the scans. They should provide the best line fluxes if the continua have been measured accurately. We have assumed the  $4 \mu\text{m}$  continuum flux densities from the references in column (5) to compute the Br $\alpha$  line fluxes in column (2); these are discussed in § IIIb. The uncertainties in the line fluxes can be found from those for the  $W_\lambda$ 's. The line fluxes are corrected for extinction in column (3)

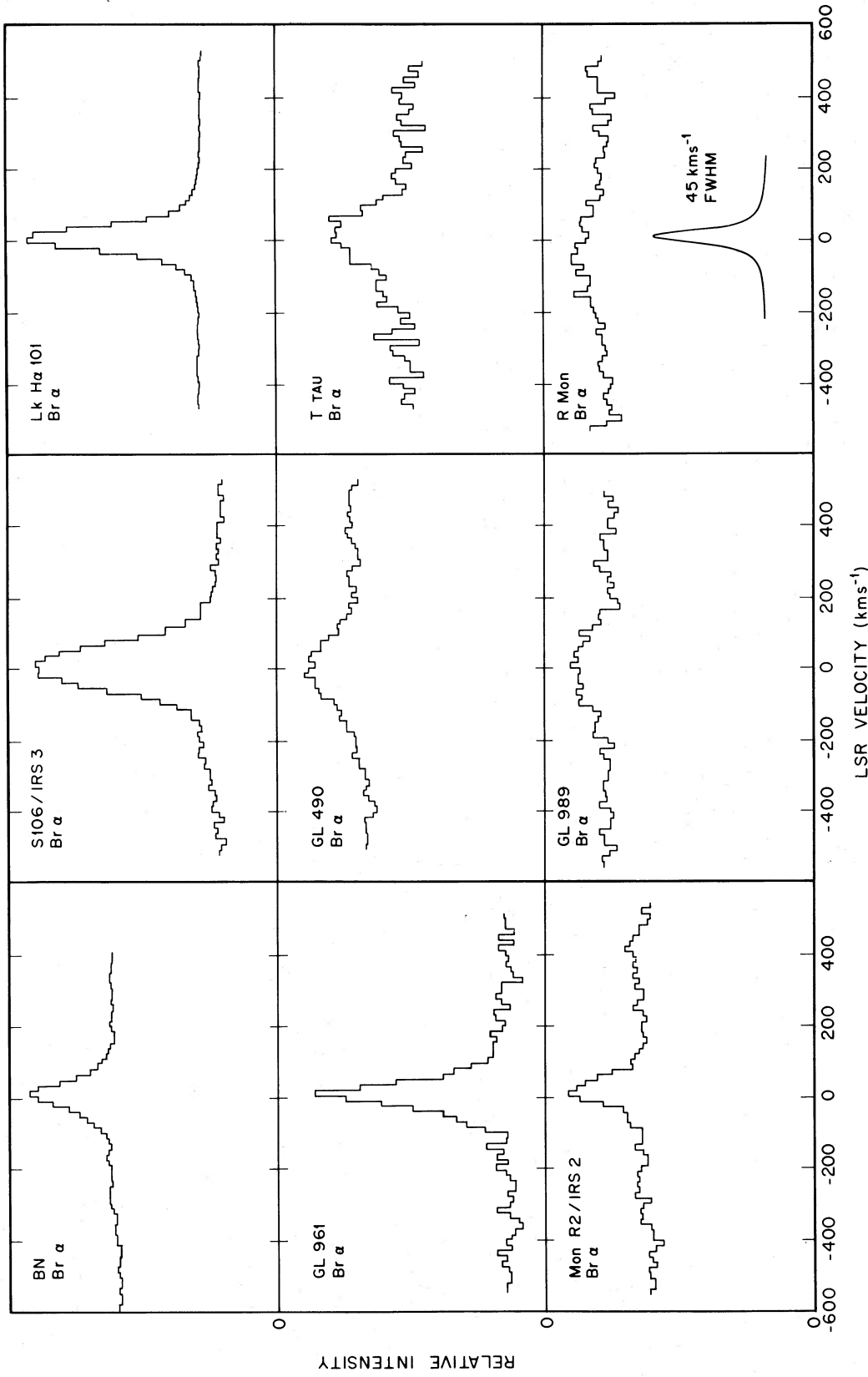


FIG. 3.—Fabry-Perot spectra of the Br  $\alpha$  line of nine YSOs obtained at the IRTF. The instrumental resolution of 45 km s<sup>-1</sup> (FWHM) is shown.

TABLE 1  
 BRACKETT-ALPHA LINE PARAMETERS FOR YSOs

Source	Flux	Corrected Flux	$W_\lambda$	Ref.	log Br $\alpha$ luminosity	FWHM Line Width	Velocity Resolution	Deconvolved FWHM	FWZI Line Width	Centroid LSR Velocity	Molecular Cloud Velocity	Ref.
(1)	( $10^{-20}$ W cm $^{-2}$ )	( $10^{-20}$ W cm $^{-2}$ )	(km s $^{-1}$ )	(5)	(W)	(7)	(8)	(9)	(km s $^{-1}$ )	(11)	(12)	(13)
BN	176	450	52 $\pm$ 10	1	26.13	106 $\pm$ 10	45	80	300	+2 $\pm$ 5	+9	8
Lk H $\alpha$ 101	1200	1626	210 $\pm$ 10	2	27.10	86 $\pm$ 10	45	60	300	-2 $\pm$ 5	-2	9
GL 490	32	46	65 $\pm$ 10	3	25.66	216 $\pm$ 15	45	190	450	-15 $\pm$ 8	-13	10
	30	43	51 $\pm$ 10	3		180 $\pm$ 20	75	135	450	-6 $\pm$ 15	-13	10
GL 961	156	252	480 $\pm$ 50	4	26.77	99 $\pm$ 10	45	75	250	+3 $\pm$ 5	+13	11
GL 989	43	(69) <sup>a</sup>	36 $\pm$ 10	1	25.72	210 $\pm$ 35	45	185	350	-8 $\pm$ 20	+8	12
Mon R2/IRS 2	27	(43) <sup>a</sup>	41 $\pm$ 10	1	25.67	93 $\pm$ 15	45	70	200	+15 $\pm$ 8	+10	13
S106/IRS 3	130	243	520 $\pm$ 30	5	26.00	152 $\pm$ 10	45	130	600	0 $\pm$ 5	-1	14
	125	234	500 $\pm$ 20	5		161 $\pm$ 20	75	115	600	+11 $\pm$ 15	-1	14
S106/A	42 $\pm$ 7	42 <sup>b</sup>	3200: <sup>c</sup>	7	...	109 $\pm$ 20	75	60	300	+6 $\pm$ 15	-1	14
S106/B	10 $\pm$ 2	10 <sup>b</sup>	700:	7	...	101 $\pm$ 20	75	50	150	+30 $\pm$ 15	-1	14
S106/C	11 $\pm$ 2	11 <sup>b</sup>	1200:	7	...	112 $\pm$ 20	75	60	200	+35 $\pm$ 15	-1	14
M17/IRS 1	36	(58) <sup>a</sup>	220 $\pm$ 30	7	26.43	177 $\pm$ 20	75	135	400	+14 $\pm$ 15	+20	15
M8E	25	(40) <sup>a</sup>	23 $\pm$ 10	4	26.03	280 $\pm$ 30	75	235	400	0 $\pm$ 20	+11	16
T Tau	32	32 <sup>a</sup>	120 $\pm$ 30	6	23.99	188 $\pm$ 20	45	160	300	-2 $\pm$ 10	+8	17
R Mon	21	21	31 $\pm$ 10	6	25.21	248 $\pm$ 50	45	225	300	-63 $\pm$ 30	+10	18

REFERENCES FOR TABLE 1.—(1) Joyce and Simon 1982. (2) Simon, Simon, and Joyce 1979. (3) Merrill, Russell, and Soifer 1976. (4) Willner *et al.* 1982. (5) Pipher *et al.* 1976. (6) Cohen 1975. (7) This paper. (8) Zuckerman, Kuiper, and Rodriguez-Kuiper 1976. (9) Knapp *et al.* 1976. (10) Lada and Harvey 1981. (11) Blitz and Thaddeus 1980. (12) Morris *et al.* 1974. (13) Loren 1977. (14) Bally and Scoville 1982. (15) Lada 1976. (16) Wright *et al.* 1977. (17) Kutner *et al.* 1982. (18) Canto *et al.* 1981.

using the  $A_V$  values derived in McGregor, Persson, and Cohen (1984). The  $A_V$  values are quite uncertain; but since  $A_{Br\alpha}/A_V \sim 0.03$ , the effects are not large. The intrinsic Br $\alpha$  luminosities in watts are given in column (6) (see below). The line widths in column (7) are the observed full widths at half-maximum (FWHM) found by fitting Gaussians to the observed line profiles. Column (9) gives the line widths after approximate removal of the effect of the instrumental profile whose FWHM values are in column (8) (75 km s $^{-1}$  at Palomar, 45 km s $^{-1}$  at IRTF). This was done by assuming (for this purpose only) that the observed line widths are Voigt functions which result from the convolution of Gaussians with the known instrumental Lorentzian. The instrumental function was thus removed to give the characteristic Gaussian FWHM values for the deconvolved line width in column (9). Column (10) gives estimates, rounded to the nearest 50 km s $^{-1}$ , for the full width at zero intensity (FWZI) of the raw spectra. Column (11) lists the LSR velocities of the line centroids, and column (12) lists the molecular cloud velocities from the literature sources in column (13).

The two measurements at the different spectral resolutions of S106/IRS 3 and of GL 490 each agree well internally. To within the uncertainties there is no difference in the observed line widths or in the equivalent widths as seen at 45 or 75 km

s $^{-1}$  resolution. The difference between the two deconvolved line widths for GL 490 (col. [9]) results from the deconvolution procedure which accentuates small differences and is susceptible to noise. The agreement in these parameters gives us confidence that the baseline slopes are not seriously affecting the line shapes or equivalent widths derived from the two other spectra obtained at 75 km s $^{-1}$  resolution—those of M8E and M17/IRS 1.

The main observational results from the figures and Table 1 are as follows:

1. All of the YSOs observed display Br $\alpha$  lines that are broader than the instrumental resolution of 45 or 75 km s $^{-1}$ . Thus among the bright infrared sources in Wynn-Williams's (1982) list that have been measured so far, we find that when the Br $\alpha$  line is detected, it is always significantly wider than the thermal line width of  $\sim 20$  km s $^{-1}$  (FWHM), and also wider than typical H I line widths in compact H II regions (S106A, B, and C provide examples; see also Geballe *et al.* 1984). Nevertheless, there appear distinct differences in the profiles from source to source. LkH $\alpha$  101, GL 961, and BN have sharply peaked profiles near line center while GL 490, GL 989, and R Mon have broad profiles that lack distinct central peaks. There is a range of a factor of 4 in the deconvolved line widths in

column (9), from  $60 \text{ km s}^{-1}$  FWHM for LkH $\alpha$  101 to  $235 \text{ km s}^{-1}$  FWHM for M8E. The large line widths and the range in character of the profiles constitute the most important observational results of the paper.

2. The Br $\alpha$  spectra of both BN and S106/IRS 3 show slight asymmetries in the sense that there is excess emission on the blue side of the line. Both of our spectra of S106/IRS 3 show the effect. There are no other sources that show any convincing Br $\alpha$  line asymmetries at the present velocity resolution. Our Br $\alpha$  profile for BN agrees with that obtained with the Fourier Transform Spectrometer at Kitt Peak and shown at a velocity resolution of  $20 \text{ km s}^{-1}$  (Scoville *et al.* 1983), though the line centroid velocities do not agree too well. Our line width value for LkH $\alpha$  101 is in reasonable agreement with that of Simon *et al.* (1984).

If, as discussed below, the Br $\alpha$  lines are optically thick and formed in an outflowing wind, then we might have expected to see self-reversals or asymmetries, as are seen in the H $\alpha$  lines in some T Tauri stars, for example. At the present spectral resolution the limits are not stringent, but there are no self-reversals in the Br $\alpha$  line with depths greater than  $\sim 30\%$  of the continuum in any source; this limit corresponds to an equivalent width of less than  $3 \text{ \AA}$  or  $22 \text{ km s}^{-1}$ .

3. The centroid velocities of Br $\alpha$  emission in all the sources except R Mon agree roughly with those of their parent molecular clouds. The broad profile of the R Mon Br $\alpha$  line makes the velocity uncertain, but at the  $2 \sigma$  level R Mon is blueshifted by  $\sim 60 \text{ km s}^{-1}$  with respect to its parent cloud.

4. The source Mon R2/IRS 2 lines some  $30''$  west of the better known source Mon R2/IRS 3 (Beckwith *et al.* 1976). We searched for Br $\alpha$  in Mon R2/IRS 3 and found none to a  $3 \sigma$  level of  $2 \times 10^{-19} \text{ W cm}^{-2}$ . This is not consistent with Simon *et al.*'s (1983) reported Br $\alpha$  flux for IRS 3. We are certain, however, that IRS 2 is significantly brighter than IRS 3 in the Br $\alpha$  line. Mohn R2/IRS 2 is embedded in an extended nebula of 10 and  $20 \mu\text{m}$  emission (Hackwell, Grasdalen, and Gehrz 1982), but the distribution of this emission is such that our measurement of IRS 2 probably underestimates the true amount of Br $\alpha$  emission. Also, the profile is considerably broader than the instrumental resolution; the deconvolved FWHM is  $\sim 70 \text{ km s}^{-1}$ . This result establishes Mon R2/IRS 2 as a member of the class of YSOs with high-density envelope characteristics and high-velocity gas flows.

We note in this connection that the  $20 \mu\text{m}$  images of the region by Hackwell *et al.* clearly show that IRS 2 lies near the center of an extended shell-like  $20 \mu\text{m}$  source which seems unrelated to IRS 3. It is possible that a wind from IRS 2 has cleared out the apparent cavity; Hackwell *et al.* also suggest that IRS 1 is a blister H II region excited by IRS 2.

5. The Br $\alpha$  lines in the three compact H II region components S106A, B, and C are considerably narrower than that of S106/IRS 3, yet the observed profiles are slightly broader than the instrumental resolution. The centroid velocities of the three components are not the same: S106A has the same velocity as S106/IRS 3 and the molecular cloud velocity, but S106B and C are both redshifted from this by  $\sim 30 \text{ km s}^{-1}$ . Direct comparison with the [S III] velocity data of Hippelin and Münch (1981) is not instructive because the angular and spectral resolutions of the two data sets are quite different. However, the two data sets are consistent in showing that the northern lobe is receding from the southern lobe (S106A).

The Br $\alpha$   $W_\lambda$  values for the S106A, B, and C are uncertain by roughly a factor of two because the continua are faint. The  $W_\lambda$

value for S106A does, however, appear to be higher than that of the other two radio condensations B and C.

7. Figure 4 shows a comparison of the Br $\alpha$  and Br $\gamma$  profiles of S106/IRS 3, M17/IRS 1, and GL 490, with linear baselines removed. The Br $\gamma$  profiles for M17/IRS 1 and GL 490 are those of Simon *et al.* (1981), broadened to our velocity resolution ( $75 \text{ km s}^{-1}$  for M17/IRS 1,  $45 \text{ km s}^{-1}$  for GL 490). The Br $\alpha$  and Br $\gamma$  line widths and profile shapes of these three sources are the same to within  $20 \text{ km s}^{-1}$ , which is within the uncertainties of our rather low resolution data.

#### b) Brackett- $\alpha$ Line fluxes

In some cases the Br $\alpha$  line flux data in Table 1 are not in particularly good agreement with values from the literature. In

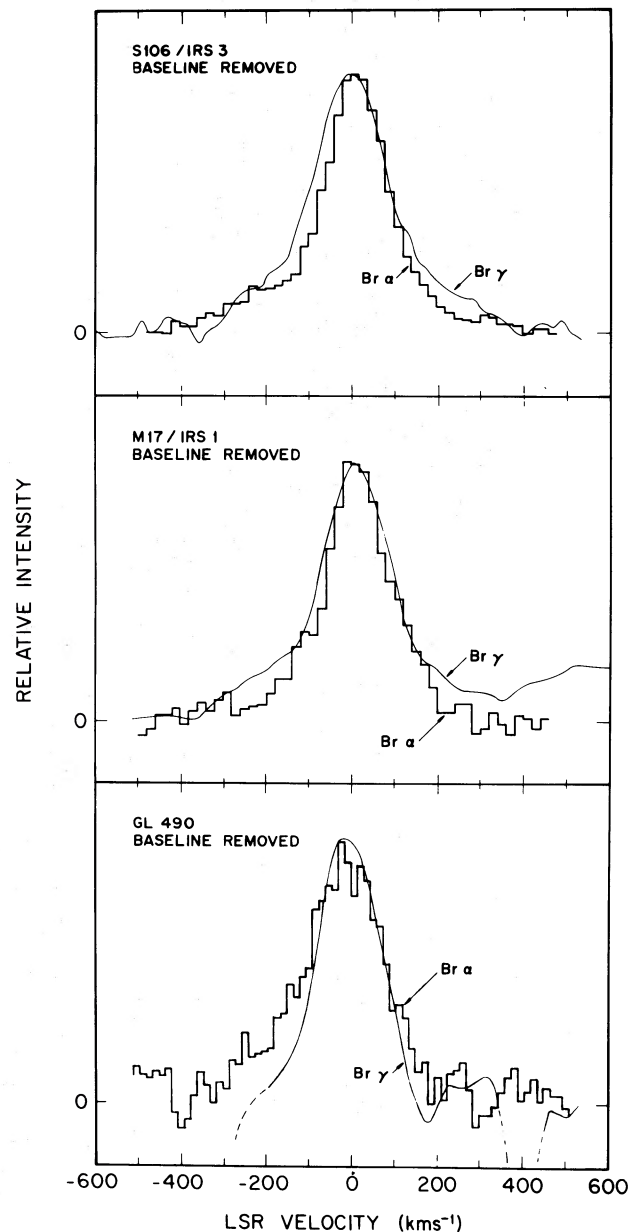


FIG. 4.—Comparison of the shapes of the Br $\alpha$  and Br $\gamma$  lines. The data for S106/IRS 3 are from Fig. 1. The Br $\gamma$  data for M17/IRS 1 and GL 490 are from Simon *et al.* (1981), smoothed to our resolutions of  $75$  and  $45 \text{ km s}^{-1}$ , respectively.

view of the importance of these fluxes and the  $\text{Br}\gamma/\text{Br}\alpha$  ratio to the interpretation of the envelope emission in terms of stellar wind (and other) models, and in determining the reddening, we now discuss the discrepant cases. First, we note that for BN, GL 490, and GL 989, the  $\text{Br}\alpha$  fluxes of various authors agree to within 10% of their average values.

For  $\text{LkH}\alpha$  101 we find a  $\text{Br}\alpha$  flux value of  $1.2 \times 10^{-17} \text{ W cm}^{-2}$ , while Joyce and Simon (1982) obtain  $2.0 \times 10^{-17} \text{ W cm}^{-2}$ . We have no explanation for this difference.

For GL 961 Simon *et al.* (1983) quote  $8 \times 10^{-19} \text{ W cm}^{-2}$ , and Simon, Simon, and Joyce (1979) quote  $12 \times 10^{-19} \text{ W cm}^{-2}$ ; both measurements were made with a beam 11" in diameter. Simon *et al.* (1983) do not comment on this discrepancy; our measurement of  $15.6 \times 10^{-19} \text{ W cm}^{-2}$  is in better agreement with the earlier data.

There is a substantial dispersion in the values for S106/IRS 3. Pipher *et al.*'s (1976) data give a flux of  $1 \times 10^{-18} \text{ W cm}^{-2}$  if corrected according to them for extended foreground emission from the bright H II region. Tokunaga and Thompson (1979), however, quote  $6.2 \times 10^{-18} \text{ W cm}^{-2}$  which we feel must be in error. Simon *et al.* (1983) obtained  $2.5 \times 10^{-18} \text{ W cm}^{-2}$  with an 11" beam. In our 6" beam we measure  $1.25 \times 10^{-18} \text{ W cm}^{-2}$ , a value which we feel is closer to the true value than that of Simon *et al.* because of the extended foreground emission. We also measure  $W_\lambda$  for the  $\text{Br}\gamma$  line to be  $400 \text{ km s}^{-1}$ . Taking the the  $2.16 \mu\text{m}$  flux density to be  $3.0 \text{ Jy}$  (Pipher *et al.* 1976; Tokunaga and Thompson 1979), we obtain a  $\text{Br}\gamma$  flux of  $5.7 \times 10^{-19} \text{ W cm}^{-2}$ , and a  $\text{Br}\gamma/\text{Br}\alpha$  ratio of  $0.46 \pm 0.10$ . Our  $\text{Br}\gamma$  flux is about 30% higher than that of Tokunaga and Thompson (1979).

For M17/IRS 1 Simon *et al.* (1983) have noted difficulties with their previous measurements; our data agree with the earlier data of Simon *et al.* (1981).

For M8E we find  $25 \pm 5 \times 10^{-20} \text{ W cm}^{-2}$ , compared to the Simon *et al.* (1981) value of  $16 \pm 3 \times 10^{-20} \text{ W cm}^{-2}$ . These data are just consistent.

#### IV. DISCUSSION

##### a) Line Strengths

The objects in the sample cover a wide range in bolometric luminosity, from T Tau at  $L/L_\odot = 37$ , to S106/IRS 3 at more than  $2 \times 10^4$ . Thompson (1982) has pointed out that for luminous YSOs  $\log(L/L_\odot)$  is nearly linearly related to  $\log N_e^2 V$  (which is derived from infrared line fluxes) and does not follow the relationship expected if the ionizations are due to normal zero-age main-sequence stars. It is of interest to extend this comparison to the lower luminosity YSOs included here and to other classes of objects.

The line luminosities (Table 1, col. [6]) are compared to the bolometric luminosities in Figure 5 where the luminosities and distances are the same as those used by Thompson (1982) except for S106, where we have adopted a distance of 600 pc (Staudte *et al.* 1982). Figure 5 extends Thompson's result: the  $\text{Br}\alpha$  luminosity is linearly related to the total luminosity over nearly four orders of magnitude. Clearly, the  $\text{Br}\alpha$  line luminosity is not directly determined by the number of ionizing photons shortward of the Lyman limit; the less luminous objects emit virtually none of their energy shortward of  $912 \text{ \AA}$ .

Simon *et al.* (1983) and Thompson (1984) have explored the possibility that ionizations from the second level of hydrogen could account for the "missing" ionizations required to maintain the flux of H I line photons. Two new facts from the work

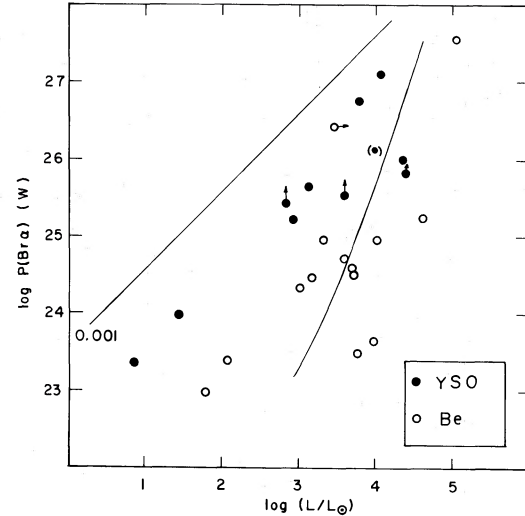


FIG. 5.—The power emitted in the  $\text{Br}\alpha$  line versus the bolometric luminosity of the YSOs (solid symbols) and a sample of Be stars (open symbols). The straight line at  $45^\circ$  is simply a fiducial line that corresponds to 0.1% of the total power emitted in the  $\text{Br}\alpha$  line. The curved line corresponds to the Lyman continuum photon output of ZAMS stars, and Case B recombination theory; see Thompson (1982).

of McGregor, Persson, and Cohen (1984) lend support to this idea. First, the high optical depths inferred for high members of the Paschen series make it likely that the optical depth through the envelope for ionizations from the  $n=2$  level could approach or exceed unity. Second, the ratio of the  $\text{O I } \lambda 8446$  line to that of  $\text{H}\alpha$  was shown to imply that the optical depth in  $\text{H}\alpha$  was  $\sim 10^3$  with an uncertainty of order a factor of 3. For  $\tau(\text{H}\alpha) = 10^3$  the optical depth at the Balmer continuum edge is  $\sim 0.1$ . Considering the uncertainties, this optical depth is close enough to unity to suggest that the Balmer continuum energy could indeed supply the ionizing photons required. A detailed solution to this problem will involve modeling the  $\text{Ly}\alpha$  radiation field and the ionization structure of the envelope, since the  $\text{O I}$  line is excited in transition regions.

McGregor, Persson, and Cohen (1984) found several similarities between the  $0.6\text{--}1.0 \mu\text{m}$  spectra of a sample of YSOs and those seen in Be stars and T Tauri stars, and thus it is of interest to compare the total amount of envelope emission in Be stars and the YSOs. Figure 5 also shows the  $\text{Br}\alpha$  luminosities for the sample of Be stars in Persson and McGregor (1984). The Be stars show a qualitatively similar relationship to the embedded sources, except that the Be star  $\text{Br}\alpha$  line luminosities are roughly a factor of 10 weaker at a given total luminosity. The Paschen, Brackett, and Pfund line emission of the Be star envelopes is, in general, optically thick, and the  $\text{O I}$  and  $\text{Ca II}$  line emission characteristics are also indicative of common physical conditions in the two types of object (see McGregor, Persson, and Cohen 1984). The curved line in Figure 5 shows the  $\text{Br}\alpha$  fluxes expected on the basis of Case B recombination theory, which clearly has nothing to do with the actual line emission in these dense envelopes, but illustrates a point that is relevant for the YSO envelopes. The relative lack of a line "excess" problem (Thompson 1981, 1982) for Be stars could be interpreted to mean that the solid angle of the envelope as seen from the stellar surface is smaller for the Be stars than the YSOs, or that the optical depth in the Balmer continuum is just enough smaller that efficient conversion of Balmer continuum energy into H I line photons is reduced. If the solid angle also

enters the situation for the YSOs, then one could expect to find dense envelope characteristics, such as have been listed above, in YSOs that do not have particularly severe line "excess" problems. S106/IRS 3 might be a case in point. All indications point to a very dense envelope: thick H I Paschen and Brackett lines, O I and Ca II emission, and an optically thick wind in the radio (Bally, Snell, and Predmore 1983). Yet its Br $\alpha$  line flux is roughly consistent with optically thin recombination emission;  $N_e^2 V = 1 \times 10^{59} \text{ cm}^{-3}$  and  $\log L/L_\odot = 4.35$  (cf. Thompson 1982). Thus we suggest that the agreement with Case B for S106/IRS 3 in the (luminosity,  $N_e^2 V$ )-diagram is an accident; the envelope is actually very optically thick in the equatorial direction, and physically thin in the vertical direction. This geometry is consistent with the extremely disklike gas and dust distribution revealed by the VLA maps of Bally, Snell, and Predmore (1983). Such a possibility would also suggest caution in concluding that other objects in the (luminosity,  $N_e^2 V$ )-diagram that do not have "excess" line emission have optically thin envelopes, in which Case B recombination theory applies. They may actually have envelopes that are optically thick to Balmer continuum photons, but only in certain directions. Presumably, these directions are equatorial; primary ionizing photons and the flow of energy and momentum emerge orthogonal to the disk plane.

In an overlapping sample of YSOs, Bally and Lada (1983) and Edwards and Snell (1983) have found the bolometric luminosities to be linearly related to both the mechanical luminosity and the momentum flux  $\dot{M}V_{\text{CO}}$  in the cool molecular outflows from these objects. The connection between the momentum flux excess, Br $\alpha$  luminosity, and total luminosity suggests that an underlying mechanism might provide the energy and momentum for the extended molecular outflows and the H I line photons. However, if the Balmer continuum ionization explanation for the Br $\alpha$  fluxes is correct, then the luminosity-line-flux relationship *can* be explained in terms of the photon output of the central star. On the other hand, the momentum flux problem cannot be because  $\dot{M}V_{\text{CO}}$  generally exceeds  $L/c$  by several orders of magnitude, as has been emphasized by several authors. This would argue against information on the momentum flux problem being found in the ionized outflowing gas close to the star. We return to this question in § IVd.

#### b) Line Widths and Shapes

The Br $\alpha$  FWHMs corrected for instrumental profile are plotted in Figure 6 as a function of stellar luminosity. The FWHMs, which range from 80 to 200  $\text{km s}^{-1}$ , are not correlated with stellar luminosity. In fact, several of the highest luminosity sources have smaller FWHMs than T Tau. The Br $\alpha$  FWZIs appear to be considerably smaller than the velocities of  $\geq 1000 \text{ km s}^{-1}$  inferred for the winds from O-B stars (see, e.g., Snow and Morton 1976) as determined from the widths of UV resonance lines. However, one cannot rule out the possibility that some gas is moving at equally large velocities in the vicinities of the YSOs, because the column densities of material needed to produce measurable Br $\alpha$  line emission above a bright  $4 \mu\text{m}$  continuum will depend strongly on the optical depth in the line wings as well as on the length and sensitivity of the spectral scan. The H $\alpha$  widths seen in Be stars tend to be wider than those in Figure 1, but again the comparison is not justified, because the optical depth in H $\alpha$  probably greatly exceeds that in Br $\alpha$ . The lack of correlation of the line widths with the stellar luminosities could be interpreted in a number

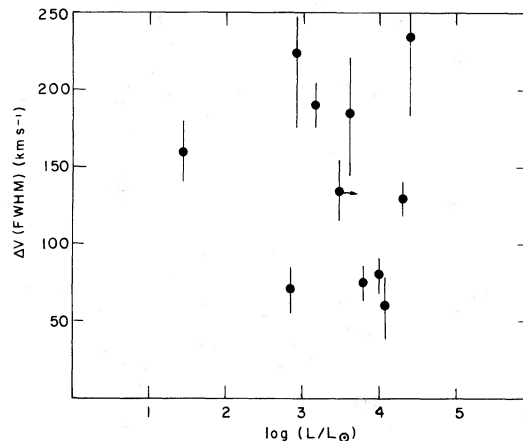


FIG. 6.—The full width at half-maximum velocity width, corrected for instrumental resolution for the 11 YSOs in Table 1.

of ways. The acceleration mechanism may operate completely independently of the source luminosity, or the point at which the optical depth reaches unity (at each point in the profile) varies from source to source within the region that the flow is accelerating or decelerating. Alternatively, perhaps rotation of the envelope plays a role, and aspect angle effects determine the profile width in part. A full interpretation will ultimately require a detailed line transfer model on a case-by-case basis.

#### c) Comparison with Wind Models

Krolik and Smith (1981) and Simon *et al.* (1981, 1983) have presented models designed to interpret the strong and wide H I lines seen in high-mass YSOs in terms of a stellar wind that is optically thick in the H I lines and in the radio continuum. Although the models are not free of assumptions about the basic nature of the flows, geometries, and line broadening mechanisms, and although they contain a basic assumption for which there is no support, viz., that the Sobolev approximation is valid over the bulk of the envelope, they do serve as a useful starting point. An important aim of these models is to derive mass loss rates  $\dot{M}$  from the line and continuum fluxes and wind terminal velocities  $V_f$ . The resulting values of  $\dot{M}V_f$  are then compared to those found for the extended molecular outflows. Before discussing this problem it is of interest to check for consistency between the Br $\alpha$  and radio continuum data in terms of the wind models. A stellar wind source can be inferred from a Br $\alpha$  plus total luminosity comparison (Thompson's "line excess" comparison); confirmation should follow from the Br $\alpha$  to radio flux ratio and the radio spectral index. Although the observed Br $\alpha$  line flux depends on extinction, a 6 mag uncertainty in  $A_v$  has only a 20% effect.

Table 2 gives the source parameters in the comparison. As will be shown below, the mass loss rates are large enough to ensure that  $\tau_{\text{Br}\alpha} > 1$ , consistent with the results of McGregor, Persson, and Cohen (1984), so the models of Krolik and Smith or Simon *et al.* can be used. Column (2) repeats the reddening-corrected Br $\alpha$  fluxes from Table 1, column (3) gives the adopted distances, and column (4) gives the 5 GHz flux predicted from the Simon *et al.* (1983; eq. [20]) formula which is valid for large  $\tau_{\text{Br}\alpha}$  and in the asymptotic limit that the recombination radius  $r_0$  is much larger than the inner radius of the shell  $r_i$ :

$$S_\nu(5 \text{ GHz}) = F_c(\text{Br}\alpha)/7.3V_{100}^{-1/3},$$

$$(\text{mJy}) \quad (10^{-12} \text{ ergs cm}^{-2} \text{ s}^{-1})$$

TABLE 2  
BRACKETT-ALPHA AND RADIO FLUX COMPARISON

Source (1)	$F_C$ (Br $\alpha$ ) ( $10^{-12}$ erg $\text{cm}^{-2}$ $\text{s}^{-1}$ ) (2)	d (kpc) (3)	$S_{\nu}$ 5 GHz (mJy) (4)		Radio Spectrum (6)	Ref. (7)	Wind Consistency for Br $\alpha$ and Radio? (8)	$\dot{M}$ ( $M_{\odot}$ $\text{yr}^{-1}$ ) (9)	$\dot{M}$ ( $M_{\odot}$ $\text{yr}^{-1}$ $\text{km s}^{-1}$ ) (10)	(L/c)/ $\dot{M}$ (11)
			predicted	observed						
BN	45	0.5	5.4*	<2	wind?	1	Yes	7.5(-7)	1.1(-4)	1.8
Lk H $\alpha$ 101	163	0.8	19.4	24.6*	wind	2	Yes	4.7(-6)	7.0(-4)	0.4
GL 490	4.6	0.9	0.48*	<1	wind?	3	Yes	4.5(-7)	1.0(-4)	0.3
GL 961	25.2	1.4	3.19	0.9 $\pm$ 0.3*	...	4	Yes	7.7(-7)	9.6(-5)	1.3
GL 989	6.9	0.8	0.80*	<12	...	5	Yes	4.3(-7)	7.5(-5)	1.1
Mon R2/IRS 2	4.3	0.95	0.60*	...	...	6	?	2.5(-7)	2.5(-5)	0.6
S106/IRS 3	24	0.6	2.28	5.4 $\pm$ 0.2*	wind	7,4	Yes	2.0(-6)	6.0(-4)	0.7
M17/IRS 1	5.8	2.5	0.63*	4	flat	3	see text	2.2(-6)	4.4(-4)	>0.1
M8E	4.0	1.5	0.43*	3.9,4.1	flat	3,8,9	see text	7.8(-7)	1.6(-4)	3.2
T Tau	3.2	0.16	0.37	0.45 $\pm$ 0.5*	wind	2	see text	1.9(-8)	2.9(-6)	0.2
R Mon	2.1	0.8	0.26*	...	...	...	?	1.6(-7)	2.4(-5)	0.7
HL Tau	0.8	0.16	0.11*	<0.4	...	10	Yes	4.9(-9)	4.9(-7)	0.3

NOTE.—Asterisks in columns (4) and (5) denote the values of  $S_{\nu}$  used to find the  $\dot{M}$  values in column (9).  
REFERENCES FOR TABLE 2.—(1) Moran *et al.* 1983. (2) Cohen, Bieging, and Schwartz 1982. (3) Simon *et al.* 1983. (4) Bally and Pridmore 1983. (5) Harris 1976. (6) Simon *et al.*, to be published. (7) Bally, Snell, and Pridmore 1983. (8) Simon *et al.* 1981. (9) Simon *et al.* 1984. (10) Bieging, Cohen, and Schwartz 1984. (11) Simon *et al.* 1981. (9) Simon *et al.* 1984. (10) Bieging, Cohen, and Schwartz 1984.

where  $V_{100}$  is one half the FWZI value in units of  $100 \text{ km s}^{-1}$  from Table 1.

The radio continuum flux densities predicted from the Krolik and Smith (1981) formulation are roughly a factor of 3 smaller than those of Simon *et al.* in the asymptotic limit of a large outer ionized radius in the wind. For smaller outer radii the Simon *et al.* radio predictions fall in closer accord with the Krolik and Smith results. Column (5) gives the observed 5 GHz radio continuum flux densities, and column (6) gives an indication of whether or not the radio spectrum is consistent with a wind energy distribution (see Panagia and Felli 1975) or a compact H II region spectrum ("flat"). The references for the entries in columns (5) and (6) are in column (7). Column (8) gives an indication of whether the predicted and observed 5 GHz flux densities are consistent with the  $\text{Br}\alpha$  fluxes in terms of a wind model, where agreement to within a factor of 2 is considered good, in view of the various assumptions made about the source geometry and density dependence on radius. The basic result from Table 2 is that the  $\text{Br}\alpha$  and radio fluxes are in agreement for the wind models, where comparisons can be made. Remarks on a few individual cases follow.

For BN the radio spectrum may be consistent with a wind (Moran *et al.* 1983); the observed  $\text{Br}\alpha$  flux is stronger than expected on the basis of the present 5 GHz upper limit. The  $\text{Br}\alpha$  and radio spectrum fit the Simon *et al.* (1983) formulation for LkH $\alpha$  101 very well. For GL 490, the predicted radio flux is faint; the present radio upper limit is consistent with the measured  $\text{Br}\alpha$  flux, but not really consistent with a 1.3 cm radio measurement (Simon *et al.* 1983) for a  $v^{0.6}$  wind spectrum. For GL 961 the measured radio flux is less than that predicted from the asymptotic form of the Simon *et al.* prediction. For GL 989 the radio data are meager, and at present the  $\text{Br}\alpha$  prediction is best. No published information on the radio flux from Mon R2/IRS 2 exists. Fair agreement pertains for S106/IRS 3, whose radio spectrum has been shown by Bally and Predmore (1983) to be well represented by a  $v^{0.6}$  relationship (they also use a  $\text{Br}\alpha$  flux that is too large (see § IIIb). In this connection it is interesting that our new value for the  $\text{Br}\gamma/\text{Br}\alpha$  ratio is in good accord with wind model predictions. Correcting the observed value of 0.46 for extinction leads to a value near unity, which is significantly different from the recombination value of 0.33, but close to values for optically thick winds (Simon *et al.* 1983).

For M17/IRS 1 no agreement should be expected as the radio spectrum is flat (see Simon *et al.* 1981, 1983). It seems probable that the source is complex, with optically thick and thin components; it is not likely that the  $\text{Br}\alpha$  flux measured is from the same volume of space as the radio flux. For M8E a similar discrepancy occurs as for M17/IRS 1. Simon *et al.* (1984) showed that the flat-spectrum 4 mJy VLA source is not positionally coincident with the IR source. The lack of radio emission from the IR source is consistent with the  $\text{Br}\alpha$  flux. T Tau is discussed in § IVe. No radio data are available for R Mon.

#### d) The $\dot{M}V$ Problem

A well-known discrepancy exists between the rate of momentum deposition  $\dot{M}V_{\text{CO}}$  in cool molecular outflows and that available from the radiation field (assuming single scattering),  $L/c$  (e.g., Bally and Lada 1983; Edwards and Snell 1983). Bally and Predmore (1983) have also compared the  $\dot{M}V_{\text{CO}}$  values to those found from consideration of the ionized mass-loss winds. Wind mass-loss rates, listed in column (9) of

Table 2, were found using the Panagia and Felli (1975) formula

$$\dot{M} = 4 \times 10^{-6} S_{\nu}^{0.75} d^{1.5} \nu^{-0.45} V_{1000},$$

( $M_{\odot} \text{ yr}^{-1}$ )                      (mJy) (kpc) (5 GHz) ( $1000 \text{ km s}^{-1}$ )

where  $V_{1000}$  is FWZI/2000 from Table 1 ( $100 \text{ km s}^{-1}$  has been assumed for HL Tau).<sup>8</sup> In each case the 5 GHz flux density used is that from a definite wind radio spectrum, or that predicted from the  $\text{Br}\alpha$  flux; the values actually used are noted with asterisks in columns (4) and (5).

The momentum deposition rates  $\dot{M}V_i$  for the ionized gas are given in column (10). These values can be compared directly with the force available in the radiation field, which is  $L/c$  under the assumption of single scattering of the photons. Column (11) gives the ratio of  $L/c$  to  $\dot{M}V_i$ .<sup>9</sup> An entry greater than unity indicates that the radiation field of the core infrared source is easily capable of driving the outflow seen at the core source itself. Note that the ratios are all within factors of a few of unity, thus indicating that if multiple photon scattering is effective enough to produce momentum deposition rates in excess of  $L/c$  by factors of a few, the *the core source radiation fields are capable of driving the ionized outflows*. Such enhancements have been discussed by, e.g., Phillips and Beckman (1980), and Faulkner (1970). The numerical "efficiency" factor here is necessarily uncertain because in addition to uncertainties in the mass loss rates and wind velocities, the geometry also enters the problem. If much of the envelope gas is in a disk, as discussed above, then it is not clear how the two momentum rates should be compared.

This result appears to differ markedly from that of Bally and Predmore (1983; column 11 in their Table 2), and it is important to clarify the situation. The difference involves the ionized wind velocities. Where we have taken measured velocities, Bally and Predmore *assumed* that the ionized wind momentum rates  $\dot{M}V_i$  equaled the values of  $\dot{M}V_{\text{CO}}$ , and have derived the ionized wind velocities required to satisfy this constraint. Our point of view is that the  $\dot{M}V_i$  values derived from the ionized gas should be used to give an independent estimate of the force available at the core source envelope. If the measured wind velocities underestimate the true terminal wind velocities by, say, a factor of 3, then the true  $\dot{M}V_i$  values will be one order of magnitude higher.

Large differences between the values of  $L/c$  and  $\dot{M}V_{\text{CO}}$  have been compiled by Bally and Lada (1983) and Edwards and Snell (1983) for many of the sources in our sample. The entries in column (11) show that the ionized gas momentum rates also fail to account for the molecular gas motions. Again, even if the true line widths are 3 times as wide as measured,  $L/c$  can probably still account for  $\dot{M}V_i$  (with multiple scattering), but the  $\dot{M}V_{\text{CO}}$  values remain unexplained. Thus we have the situation that the force in the ionized component of the wind close to the core sources (on a scale of  $\sim 10^{13}$  cm) can be supplied by the radiation field, but that at larger distances (up to the parsec scale) a significantly larger force is required.<sup>10</sup>

<sup>8</sup> The mass-loss rates in column (9) were found with our values of  $V$ . We do not see evidence for the large value used by Cohen, Bieging, and Schwartz (1982) for LkH $\alpha$  101, but the column (9) values are certainly lower limits. We note that for all the sources except HL Tau the mass loss rates are consistent with high optical depth in the  $\text{Br}\alpha$  line: for  $\dot{M} = 10^{-6} M_{\odot} \text{ yr}^{-1}$ ,  $\tau_{\text{Br}\alpha}$  at line center  $> 3 \times 10^4$  in LTE.

<sup>9</sup> The Table 2 entries for T Tau refer to the optical object, not the infrared companion. See § IVe.

<sup>10</sup> A possible exception is NGC 7538/IRS 1, discussed by Campbell and Thompson (1984).

It is natural to assume that the core infrared sources do somehow supply the much larger momentum requirement of the extended outflows, and the key question to be answered then is whether they do so continuously or in bursts. As the conclusion that bursts are *required* would clearly be far-reaching, it is essential to explore possible continuous driving mechanisms. It is important to note that the momentum flux in the ionized wind is a lower limit to the total that might actually be available, for example in neutral gas (Bally and Predmore 1983). The presence of strong O I  $\lambda$ 8446 emission in many YSOs (McGregor, Persson, and Cohen 1984) indicates that there is considerable neutral material present, and shows that this mechanism certainly remains viable. A possible geometry for the neutral gas is that it is swept along in the outflowing ionized gas in dense filaments. However, one should not then expect agreement between the radiative momentum rate  $L/c$  (or a few times  $L/c$ ) and the  $\dot{M}V_I$  values, as the neutral material must carry the bulk of the force. If the neutral gas emission arises at a spherically symmetric recombination front outside the ionized zone, then it can be relevant to the problem only if it can be shown that a further acceleration is occurring there. A final possibility is that the acceleration needed for the extended outflows occurs in a neutral zone that is unobservable.

Several models have been advanced to explain the  $\dot{M}V_{CO}$  problem, under the assumption that the outflows are continuous. The mechanisms generally involve tapping the supply of rotational or magnetic energy of the YSO. It is important to attack the  $\dot{M}V$  problem concurrently with the interpretation of the emission-line strengths and profiles, as the entire flow pattern and run of physical conditions in the flow must result directly from the forces on the material in the wind. Hartmann, Edwards, and Avrett (1982) have discussed an Alfvén wave-driven wind model for the lower luminosity T Tauri stars. In this class of model the width of the H I lines is due to transverse motion of gas responding to the outwardly propagating Alfvén waves. The resulting line shapes are highly dependent upon the turbulent broadening in the gas, especially for the H $\alpha$  line, for which the optical depth can be very large and the Sobolev approximation is not valid. The impact of wave-driven winds on outflows from high-luminosity objects has not been examined, but the similarities in envelope properties across a range of several orders of magnitude in luminosity suggest that a connection could exist.

Draine (1983) has advanced a mechanism whereby rotation of the YSO causes a frozen-in magnetic field to wind up above the poles of the star. The increased magnetic energy density then causes material to expand away from the star in a bipolar flow. This model does not involve collimation by the surrounding medium, as in the model developed by Königl (1982). In either of these models asymmetric line shapes might be expected as a result of differential extinction through the disk material, depending on the geometry.

Hartmann and MacGregor (1982) have discussed a rotationally driven wind model whereby the mass loss occurs mainly at the equator of a rapidly rotating star. In this case, the interaction of the wind with the surrounding material would have to redirect the flow.

Recently, Pudritz and Norman (1983) have developed a model in which the rotational energy of a protostar is set equal to the energy requirement of the cool wind. Ionized material rotating around the core slides outward along magnetic field lines which have been constricted by the earlier collapse. If this type of model could be applied to the size scales in question

here, viz.,  $10^{13}$  cm, rather than the  $10^{16}$  cm scale considered by Pudritz and Norman, it would certainly be attractive because the problem of the outward transport of angular momentum is addressed and solved at the same time. It is intriguing to speculate that the wide lines observed do indeed contain a substantial rotation plus radial component in the equatorial plane as a result of angular momentum transfer that *must* occur before the star settles down on the main sequence. Line profiles for these classes of model would be instructive.

#### e) T Tauri

For T Tau a comparison of the H $\alpha$  and Br $\alpha$  line profiles can be made, thus allowing a probe of the structure and dynamics of the wind from this young star. It is of particular interest to attempt to isolate the contribution to the Br $\alpha$  line flux from the recently discovered close binary companion to T Tau (Dyck, Simon, and Zuckerman 1982). The southern, cool, low-luminosity embedded source is the dominant contributor to the radio continuum emission from the region (Schwartz *et al.* 1984), but is fainter at all near-infrared wavelengths (contrary to the original suggestion of Dyck *et al.*). The expanding molecular outflow centered on the binary pair indicates that an energetic wind is driven from one or both of the sources (Edwards and Snell 1982). The H $\alpha$  profile of T Tau itself is known to be time variable, particularly in the prominence of the P Cygni structure (Kuhi 1964; Schneeberger *et al.* 1979; Hartmann 1982).

In Figure 7 is plotted the Br $\alpha$  profile of T Tau (from Fig. 1) superposed on two H $\alpha$  profiles taken several years apart. The line ratio is H $\alpha$ /Br $\alpha$  = 15. The line profiles are sufficiently similar in velocity structure, given the nonsimultaneity of the observations and the lower optical depth of the Br $\alpha$  line, to suggest that the observed Br $\alpha$  line arises from the optical object rather than the infrared companion. This is also consistent with the Br $\alpha$  flux, as the predicted 5 GHz flux density of 0.37 mJy (from the Br $\alpha$  flux, col. [4] of Table 2) agrees well with the 0.45 mJy observed (Schwartz *et al.* 1984). Thus a wind model works for T Tau(N), and indeed a  $v^{0.6}$  spectrum is consistent with the observed flux distribution.

For the southern cool companion, however, a problem arises. The radio data are well fitted by a wind spectrum (Cohen, Bieging, and Schwartz 1982; Schwartz *et al.* 1984), and thus the 4.3 mJy flux observed predicts a Br $\alpha$  flux from the

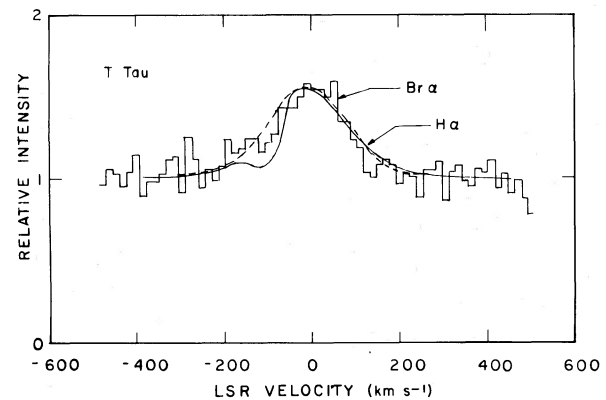


FIG. 7.—The Br $\alpha$  profile of T Tau (from Fig. 3) plotted with two H $\alpha$  profiles reproduced from Schneeberger *et al.* (1979) (solid line) and Hartmann (1982) (dashed line), and scaled to the flux at the Br $\alpha$  line peak. The Br $\alpha$  data have been binned into 15 km s $^{-1}$  intervals from the original resolution of 45 km s $^{-1}$ .

companion of  $\sim 31 \times 10^{-12}$  ergs  $\text{cm}^{-2} \text{s}^{-1}$ . Assuming that most of the observed Br $\alpha$  flux of  $3.2 \times 10^{-12}$  ergs  $\text{cm}^{-2} \text{s}^{-1}$  is from T Tau(N), the discrepancy exceeds a factor of  $31/3.2 \approx 10$ , probably by at least a factor of 2, but quite uncertain. Thus the asymptotic relationship between Br $\alpha$  and 5 GHz fluxes predicts a Br $\alpha$  flux that is roughly 20 times larger than observed. The ratio of predicted Br $\alpha$  flux to 5 GHz flux density *increases* away from the asymptotic limit in Simon *et al.*'s (1983) theory, so the solution to the problem probably does not involve the geometry. In order for extinction to account for this factor, the  $A_V$  value toward T Tau(S) would be  $\sim 100$  mag, which is larger than a recent estimate by Bertout (1983), but does not seem unreasonable given present uncertainty over the nature of this source (e.g., Bertout 1983, 1984; Hanson, Jones, and Lin 1983). It is not inconsistent with the 2–5  $\mu\text{m}$  energy distribution, if the intrinsic distribution goes as  $v^2$ .

Finally we note that if our assumption about the Br $\alpha$  flux is wrong, and nearly all of it comes from T Tau(S), then *both* sources are discrepant in their radio/Br $\alpha$  ratios.

#### V. CONCLUSIONS

Broad Br $\alpha$  emission lines have been found in 11 young stellar objects, many of which are known from radio and optical data to be sources of powerful stellar winds. The Br $\alpha$  line widths allow an estimate of the wind velocities in the region where the Br $\alpha$  line is formed, although rotation of a circumstellar disk or turbulent motions may also contribute to the line widths. The Br $\alpha$  line widths are not correlated with the bolometric luminosity of the infrared source. However, the line luminosities are found to be linearly correlated with bolo-

metric luminosity over nearly four orders of magnitude and exceed the analogous relationship for Be stars by an order of magnitude.

The Br $\alpha$  fluxes and velocity widths are consistent with radio continuum fluxes and wind models for most of the sources. The momentum deposition rates found from the source luminosities, i.e.,  $L/c$ , are within factors of a few of being able to drive the ionized outflows; and if the photons are multiply scattered, it is possible that the ionized winds are driven by radiation pressure. Thus it now appears that both the "line excess" problem and the "momentum rate" problem *for the ionized wind* can be explained in terms of the photon output of the central object. The momentum rate problem for the extended molecular outflows remains.

The Br $\alpha$  flux from the T Tau system is far weaker than expected on the basis of the radio flux from the cool companion T Tau(S), although a wind model works well for the optical object T Tau(N). This finding points to unique circumstances in envelope of T Tau(S).

This work was supported by the National Science Foundation. We are grateful to the staffs of Mauna Kea Observatory and of Palomar Observatory for their help in making the observations. We especially thank our collaborator Dr. F. Baas of Leiden University for producing the microcomputer which forms an essential part of the data system, and Dr. J. Trauger of Caltech for coating the Fabry-Perot mirrors. We also thank Drs. G. Neugebauer and J. H. Lacy for assistance with the Palomar observations. S. E. was supported in part by travel funds from the Small Grants Awards of the AAS.

#### REFERENCES

- Bally, J., and Lada, C. J. 1983, *Ap. J.*, **265**, 824.  
 Bally, J., and Predmore, R. 1983, *Ap. J.*, **265**, 778.  
 Bally, J., and Scoville, N. Z. 1982, *Ap. J.*, **255**, 497.  
 Bally, J., Snell, R. L., and Predmore, R. 1983, *Ap. J.*, **272**, 15.  
 Beckwith, S., Evans, N. J., II, Becklin, E. E., and Neugebauer, G. 1976, *Ap. J.*, **208**, 390.  
 Bertout, C. 1983, *Astr. Ap.*, **126**, L1.  
 ———. 1984, preprint.  
 Bieging, J. H., Cohen, M., and Schwartz, P. R. 1984, preprint.  
 Blitz, L., and Thaddeus, P. 1980, *Ap. J.*, **241**, 676.  
 Campbell, B., and Thompson, R. I. 1984, *Ap. J.*, **279**, 650.  
 Canto, J., Rodriguez, L. F., Barral, J. F., and Carral, P. 1981, *Ap. J.*, **244**, 102.  
 Cohen, M. 1975, *A. J.*, **80**, 125.  
 Cohen, M., Bieging, J. H., and Schwartz, P. R. 1982, *Ap. J.*, **253**, 707.  
 Draine, B. T. 1983, *Ap. J.*, **270**, 519.  
 Dyck, H. M., Simon, T., and Zuckerman, B. 1982, *Ap. J. (Letters)*, **255**, L103.  
 Edwards, S., and Snell, R. L. 1982, *Ap. J.*, **261**, 151.  
 ———. 1983, *Ap. J.*, **270**, 605.  
 Faulkner, D. J. 1970, *Ap. J.*, **162**, 513.  
 Geballe, T. R., *et al.* 1984, in preparation.  
 Gehrz, R. D., Grasdalen, G. L., Castelaz, M., Gullixson, C., Mozurkewich, D., and Hackwell, J. A. 1982, *Ap. J.*, **254**, 550.  
 Grasdalen, G. L. 1976, *Ap. J. (Letters)*, **205**, L83.  
 Hackwell, J. A., Grasdalen, G. L., and Gehrz, R. D. 1982, *Ap. J.*, **252**, 250.  
 Hanson, R. B., Jones, B. F., and Lin, D. N. C. 1983, *Ap. J.*, **270**, L27.  
 Harris, S. 1976, *M.N.R.A.S.*, **174**, 601.  
 Hartmann, L. 1982, *Ap. J. Suppl.*, **48**, 109.  
 Hartmann, L., Edwards, S., and Avrett, E. 1982, *Ap. J.*, **261**, 279.  
 Hartmann, L., and MacGregor, K. B. 1982, *Ap. J.*, **259**, 180.  
 Hippelin, H., and Münch, G. 1981, *Astr. Ap.*, **99**, 248.  
 Israel, F. P., and Felli, M. 1976, *Astr. Ap.*, **63**, 325.  
 Joyce, R. R., and Simon, T. 1982, *Ap. J.*, **260**, 604.  
 Knapp, G. R., Kuiper, T. B. H., Knapp, S. L., and Brown, R. L. 1976, *Ap. J.*, **206**, 443.  
 Königl, A. 1982, *Ap. J.*, **261**, 115.  
 Krolik, J. H., and Smith, H. A. 1981, *Ap. J.*, **249**, 628.  
 Kuhl, L. V. 1964, *Ap. J.*, **140**, 1409.  
 Kutner, M. L., Leung, C. M., Machnik, D. E., and Mead, K. N. 1982, *Ap. J. (Letters)*, **259**, L35.  
 Lada, C. J. 1976, *Ap. J. Suppl.*, **32**, 603.  
 Lada, C. J., and Harvey, P. M. 1981, *Ap. J.*, **245**, 58.  
 Loren, R. B. 1977, *Ap. J.*, **215**, 129.  
 McGregor, P. J., Persson, S. E., and Cohen, J. G. 1984, *Ap. J.*, submitted.  
 Merrill, K. M., Russell, R. W., and Soifer, B. T. 1976, *Ap. J.*, **207**, 763.  
 Moran, J. M., Garay, G., Reid, M. J., Genzel, R., Wright, M. C. H., and Plambeck, R. L. 1983, *Ap. J. (Letters)*, **271**, L31.  
 Morris, M., Palmer, P., Turner, B. E., and Zuckerman, B. 1974, *Ap. J.*, **191**, 349.  
 Panagia, N., and Felli, M. 1975, *Astr. Ap.*, **39**, 1.  
 Persson, S. E., Geballe, T. R., and Baas, F. 1982, *Pub. A.S.P.*, **94**, 381.  
 Persson, S. E., and McGregor, P. J. 1984, in preparation.  
 Phillips, J. P., and Beckman, J. E. 1980, *M.N.R.A.S.*, **193**, 245.  
 Pipher, J. L., Sharpless, S., Savedoff, M. P., Kerridge, S. J., Krassner, Schurmann, S., Soifer, B. T., and Merrill, K. M. 1976, *Astr. Ap.*, **51**, 255.  
 Pudritz, R. E., and Norman, C. A. 1983, *Ap. J.*, **274**, 677.  
 Schneeberger, T. J., Worden, S. P., and Wilkerson, M. S. 1979, *Ap. J. Suppl.*, **41**, 369.  
 Schneider, S. E., Terzian, Y., Purgathofer, A., and Perinotto, M. 1983, *Ap. J. Suppl.*, **52**, 399.  
 Schwartz, P. R., Simon, T., Zuckerman, B., and Howell, R. R. 1984, preprint.  
 Scoville, N. Z., Hall, D. N. B., Kleinmann, S. G., and Ridgway, S. T. 1983, *Ap. J.*, **275**, 201.  
 Simon, M., Cassar, L., Felli, M., Fischer, J., Massi, M., and Sanders, D. 1984, preprint.  
 Simon, M., Felli, M., Cassar, L., Fischer, J., and Massi, M. 1983, *Ap. J.*, **266**, 623.  
 Simon, M., Righini-Cohen, G., Fischer, J., and Cassar, L. 1981, *Ap. J.*, **251**, 552.  
 Simon, T., Simon, M., and Joyce, R. R. 1979, *Ap. J.*, **230**, 127.  
 Snow, T. P., Jr., and Morton, D. C. 1976, *Ap. J. Suppl.*, **32**, 4.  
 Staude, H. J., Lenzen, R., Dyck, H. M., and Schmidt, G. D. 1982, *Ap. J.*, **255**, 95.

- Thompson, R. I. 1981, in *IAU Symposium 96, Infrared Astronomy*, ed. C. G. Wynn-Williams and D. P. Cruikshank (Dordrecht: Reidel), p. 153.  
———. 1982, *Ap. J.*, **257**, 171.  
———. 1984, preprint.
- Tokunaga, A. T., and Thompson, R. I. 1979, *Ap. J.*, **233**, 127.
- Willner, S. P., et al. 1982, *Ap. J.*, **253**, 174.
- Wright, E. L., Lada, C. J., Fazio, G. G., and Kleinmann, D. E. 1977, *A.J.*, **82**, 132.
- Wynn-Williams, C. G. 1982, *Ann. Rev. Astr. Ap.*, **20**, 587.
- Zuckerman, B., Kuiper, T. B. H., and Rodríguez-Kuiper, E. N. 1976, *Ap. J. (Letters)*, **209**, L137.

SUZAN EDWARDS: Five College Astronomy Department, Smith College, Clark Science Center, Northampton, MA 01063

T. R. GEBALLE: United Kingdom Infrared Telescope, 900 Leilani Street, Hilo, HI 96720

CAROL J. LONSDALE: Jet Propulsion Laboratory, Caltech 264-338, 4800 Oak Grove Drive, Pasadena CA 91109

P. J. MCGREGOR: Mount Stromlo and Siding Spring Observatories, Private Bag, P.O. Woden ACT 2606, Australia

S. E. PERSSON: Mount Wilson and Las Campanas Observatories, Carnegie Institution of Washington, 813 Santa Barbara Street, Pasadena, CA 91101